Near-Surface Measurements of Quasi-Lagrangian Velocities in Open Water[1]

J. H. CHURCHILL AND G. T. CSANADY

Woods Hole Oceanographic Institution, Woods Hole, MA 02543

(Manuscript received 20 September 1982, in final form 31 May 1983)

ABSTRACT

Near-surface water velocities have been measured in the coastal zone of Lake Huron and Cape Cod Bay by tracking drifters and drogues using acoustic travel time and compass sighting techniques. The near-surface current, defined as the velocity of near-surface drifters and drogues relative to a drogue set at 1.8 m, varied on the depth scale on the order of 1 m, and was directed nearly parallel to the wind and to predominant wave propagation velocity. Velocity profiles were logarithmic with depth to order 1 m depth, and realistic values of stress were calculated using a law of the wall formula and a Kármán's constant of 0.4. Inferred roughness lengths were of the order of 30 cm. Anomalously high values of wind stress were inferred from velocity profiles observed during conditions of light wind and steady swell. These may be due to the similarity of Stokes drift distribution to turbulent shear flow profiles.

1. Introduction

At present, the dynamics of near-surface currents is poorly understood, partly because of the lack of field observations. Water velocity measurements using conventional current meters in the very near-surface layer are hampered by the effects of surface waves and of the supporting ship or buoy. Typically, near-surface currents are measured by tracking tracers such as drifters, drogues or dye.

We have carried out drogue and drifter tracking experiments at a number of locations, utilizing two techniques. One technique involved taking simultaneous compass sightings on drogues and drifters from two anchored vessels. The other method used an acoustic navigation system to track drogues outfitted with hydrophones and VHF transmitting equipment.

Three studies have been documented in detail. In April 1979, drogues were tracked acoustically at deep water dumpsite No. 106, ~200 km southeast of New York City (Churchill *et al.*, 1981). Compass sighting experiments were carried out in Cape Cod Bay during July 1979 (Churchill and Pade, 1980). During July and August of 1980, both techniques were used for tracking drogues and drifters in the coastal waters of Lake Huron (Churchill and Pade, 1981). The foregoing reports will be referred to as CPP81, CP80 and CP81, respectively. The measurement and data analysis techniques were slightly different for separate experiments. Those described here in detail were used in the Lake Huron project.

[1] Woods Hole Oceanographic Institution Contribution No. 5239.

2. Compass tracking experiments

a. Measurement technique

Drifters, drogues and silicon treated confetti were tracked by the method of simultaneous compass bearings. A material of densely entwined rubberized strands, "synthetic horsehair," was used for drogue and drifter construction. This material, often used as packing matter, is slightly negatively buoyant and offers a large contact surface to the water. The surface drifter consisted of a slab of the synthetic horsehair with a thin pad (~4 mm thick) of Dupont microfoam glued to the top. It was designed to drift with the horsehair material completely submerged and the pad just at the surface. The slab was of horizontal dimensions 20 cm × 20 cm, a size found to be large enough to filter out small-scale turbulence but small enough so that the drifter freely rode larger waves. Five different thicknesses (2.4, 5.0, 7.6, 10.2 and 20.4 cm) were used. The drogue was a 40.5 cm diameter by 11 cm disk of horsehair material which was submerged at a specific depth and supported at the surface by a sealed plastic shell (5.5 cm maximum diameter × 8 cm length).

In the ensuing analysis, it will be assumed that drifters and drogues followed the mean water motion at a particular depth relative to the moving surface without slippage and were stable in all wave fields experienced. Qualitative observations have indicated that these are reasonably good assumptions.

One of the vessels used for tracking will be referred to as the command ship. The other was a small, maneuverable outboard used for drogue release and re-

© 1983 American Meteorological Society

trieval (release ship). A typical tracking session proceeded as follows:

Upon arrival at the experimental site, the command ship either set anchor or tied up to a moored station. A drogue was then deployed from the command ship, and its bearing measured. The release ship was anchored so that the baseline between the two vessels was 30–45° relative to the drogue's trajectory. As demonstrated by CP80 such an orientation is optimal for relatively low uncertainty in the determination of drogue position and velocity.

Prior to each run the baseline's length and orientation were measured from both boats using telescoping rangefinders and hand-held compasses. A run commenced with the release of a double handful of confetti. Drifters and drogues were then released in order of increasing depth, with three to five deployed at each depth. Simultaneous hand-held compass bearings were taken on the confetti, clusters of drifters of the same thickness, and clusters of drogues set at the same depth. Generally they were tracked for a distance of 100–200 m, and 2–5 cycles of sightings were completed before the drogues drifted out of visual range. At the completion of tracking, the baseline was again measured from both vessels. Before and after each run, wind direction and speed at 3 m were measured.

b. Data analysis

Fig. 1 illustrates the sighting of a cluster of drifters or drogues at location d by two ships at positions 1 and 2 (release and command ships, respectively). The baseline length ($D12$) and its orientation (β_{12} and β_{21}) are taken as averages of the values measured before and after each run. The bearings α_1 and α_2 were taken simultaneously. If the sighting takes place at a time T after the cluster's release, then the speed since release is

$$SP = \frac{D1d}{T} = \frac{D12}{T}\frac{\sin(A2)}{\sin(A1 + A2)}, \quad (1)$$

where $A1$ and $A2$ are the cluster bearings with respect to the baseline. The drogue/drifter cluster direction of travel is α_1 plus the local magnetic deviation.

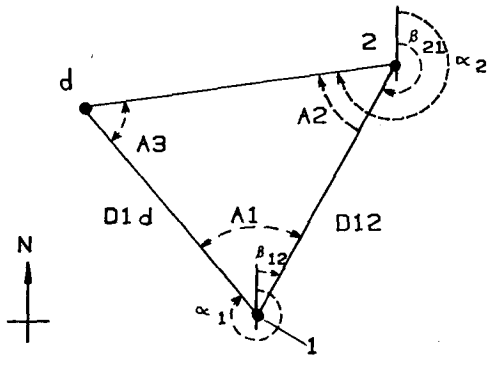

FIG. 1. Drogue sighting geometry.

Representative speed and direction of each cluster have been calculated as average values. Direction measurements were of equal reliability and have been averaged without weights. The mean speed has been calculated with weights inversely proportional to the approximate error of each value. As shown by CP81, the compass related contribution to speed error was primarily due to uncertainty in $A2$. The error due to a 1° uncertainty in $A2$ will be termed ERR2 and, to a first order approximation, is

$$ERR2 = \frac{\partial SP}{\partial A2} = \frac{\pi}{180}\frac{D12}{T}\frac{\sin(A1)}{\sin^2(A1 + A2)}. \quad (2)$$

The mean speed has been calculated as

$$\overline{SP} = \sum_{i=1}^{N} SP_i W_i \Big(\sum_{i=1}^{N} W_i\Big)^{-1}, \quad (3)$$

where N is the number of sightings on the drogue/drifter cluster during the run; SP_i the speed since release at sighting i; and $W_i = 1/ERR2_i$.

In the results to follow, the mean speed of a drogue or drifter cluster will be used as an estimate of the water velocity at the mean depth of the drogues or drifters. For drifters, this is at one-half the drifter thickness.

c. Experiment error

The rangefinders used for baseline measurements are accurate to 10% of the measured distance. As can be seen from (1), this translates to a 10% error in drogue speed.

The error in $A2$ ranged from 3° to 8° (increasing with sea state). Mean values of $ERR2$ (weighted as mean speed) ranged from 0.1 cm (s deg)$^{-1}$ to 0.4 cm (s deg)$^{-1}$. The compass related contribution to speed error thus approximately ranged from 0.3 to 3.2 cm s^{-1}. A representative value would be 1.5 cm s^{-1}.

The error in drogue/drifter bearing α_1 ranged from 2 to 5° (again, increasing with sea state).

d. Results

In Cape Cod Bay, experiments were conducted 6 km from shore in water of 24 m depth. The temperature gradient measured at this site was relatively small in the upper 5 m (~0.2°C m^{-1}) and large (1–3°C m^{-1}) from 5 to 10 m. Three typical hodographs of drogue and drifter velocities are shown in Fig. 2. Note that velocities rotated both clockwise and counterclockwise with depth. Velocities on 19 July rotated clockwise with time at approximately the tidal rate. Apparent in all hodographs are relative velocity profiles, which from deeper to shallow tracers were directed roughly parallel with the wind. (In this paper, relative velocity is defined as the vector difference

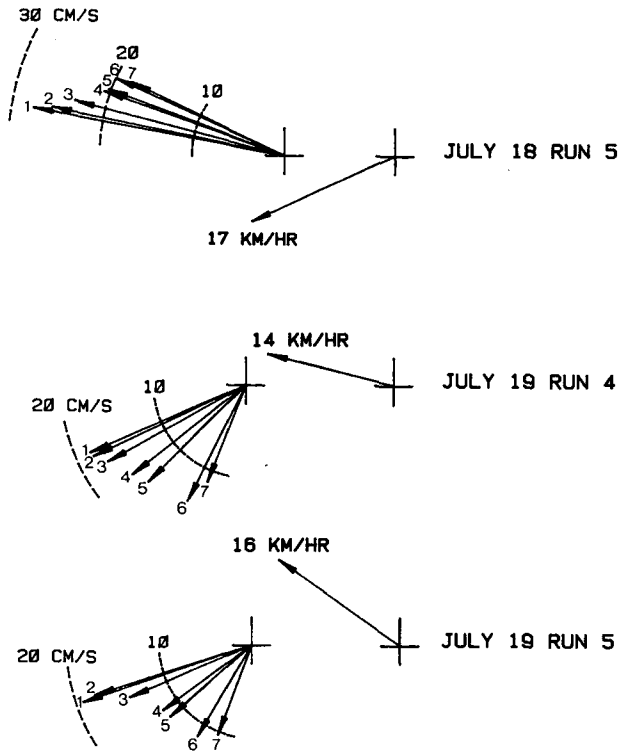

FIG. 2. Drifter, drogue and wind velocities measured in Cape Cod Bay. Vectors 1–7 refer to drifters of mean depth: 2.5 cm, 5 cm and 10 cm; and drogues of mean depth: 30 cm, 60 cm, 1.2 m and 1.8 m, respectively.

between velocities directed from the deeper to the shallower velocity. The magnitude and direction can be roughly deduced from the hodographs.)

The project site at Lake Huron is mapped in Fig. 3. The majority of the experiments were done at Station 4 which was 4 km from shore. During the project the mixed-layer depth ranged from 10 to 14 m, with a strongly stratified thermocline below (1–3°C m^{-1}). Three representative hodographs are shown in Fig. 4. As in Cape Cod Bay, velocities rotated both clockwise and counterclockwise with depth, and relative velocities were approximately parallel with the wind direction. The velocity of the shallowest drifter relative to the deepest drogue (1.2 cm and 1.8 m mean depths) was an average of 10° counterclockwise from the wind direction, with a standard deviation of 18.5°. (Due to the limited fetch the wind and wave propagation directions at both project sites were approximately the same. Thus, relative velocities were also nearly parallel with the direction of predominant wave propagation.)

It should be noted that few trustworthy fixes were taken on confetti. This is because the confetti cloud tended to become unrecognizable due to spreading and sinking before a reliable bearing could be taken from both vessels. Strictly visual observations from the release ship, however, indicated that the confetti did not travel appreciably faster than the shallowest drifters. On calm days, surface confetti was sometimes observed near the shallowest drifters while the latter were being retrieved.

During periods of steady wind, all velocities at Lake Huron were approximately in the prevailing wind direction (such as 24 July, run 2 of Fig. 4). Velocities measured shortly after a significant shift in wind direction displayed noticeable rotation with depth. On such occasions the surface velocity was nearly parallel with the existing wind and deeper velocities rotated toward the direction of strong winds during previous days (23 July, run 5 of Fig. 4, for example). The velocity at ~8 m depth, concurrently measured by a suspended, moored current meter, was approximately aligned with the longshore component of strong winds during previous days.

The foregoing observations suggest that the drogue and drifter velocities were an approximate superposition of two components: a surface-layer current, which is roughly defined by the relative velocity profile, approximately parallel with the wind and wave direction and which varies on a depth scale of about 1 m; and a subcurrent which varies on a depth scale much larger than the surface-layer current. A similar current structure with shear flow, directed parallel with the wind, superimposed on barotropic flow, was observed by Kenney (1977) from drogue studies in the Lake of the Woods.

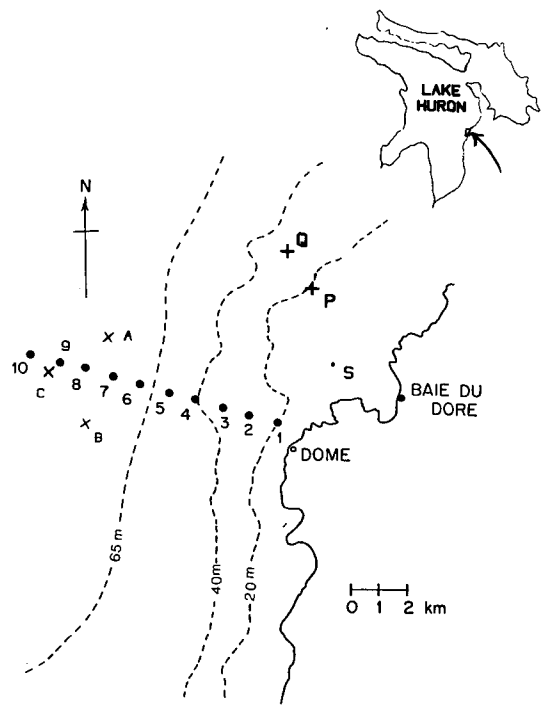

FIG. 3. Lake Huron project site. Circles 1–10 mark flag stations; the numbers are equivalent to the distance of the station from shore in kilometers. X's labeled A, B and C show bottom transponder locations.

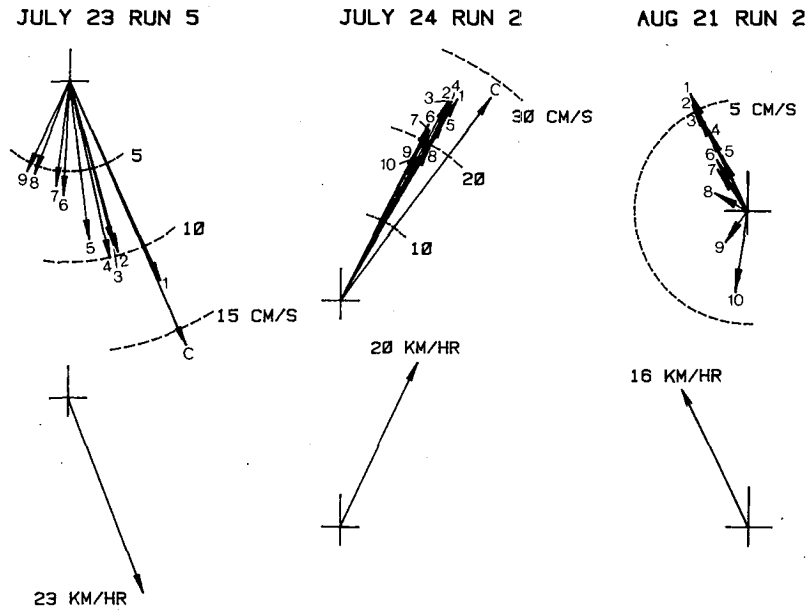

FIG. 4. Drifter, drogue and wind velocities measured in Lake Huron. Vectors 1–10 refer to drifters of mean depth: 1.2 cm, 2.5 cm, 3.8 cm, 5.1 cm and 10.2 cm; and drogues of mean depth 20 cm, 30 cm, 60 cm; 1.2 m and 1.8 m, respectively (C is confetti).

At Cape Cod Bay subcurrents were predominantly tidal. Subcurrents observed in Lake Huron were nearly parallel with the longshore component of previous strong winds and presumably generated by these winds. Such shore-parallel currents generated by persistent wind are well-known in the Great Lakes (Csanady, 1981). They are confined to a region from shore of the order of one radius of deformation width, which is typically about 5 km. Characteristics of the coastal flow at the Lake Huron project site are described in detail by Murthy and Dunbar (1981) and by CP81.

3. Acoustic tracking experiments

a. Acoustic navigation system

During these experiments, drifters and drogues equipped with sonobuoys were tracked, using an acoustic navigation system which measured travel times of pulses transmitted from three bottom mounted transponders to a hydrophone attached to the drogue or drifter. The navigation system has been employed by Woods Hole Oceanographic Institution investigators for a number of years and is well documented (Hunt *et al.*, 1974; Spindel and Porter, 1974). The system, roughly sketched in Fig. 5, consists of:

1) A transducer lowered from the tracking ship.
2) Three bottom-mounted transponders.
3) A drogue connected to a listening hydrophone and transmitting VHF antenna.
4) A receiving antenna aboard ship.
5) A shipboard minicomputer system which controls operation, processes and records incoming data, and displays computed positions.

The system operates in two phases of navigation, "ship" and "sonobuoy," which are performed as separate cycles.

The ship cycle is initiated with a pulse transmission (7.5 kHz, 10 ms) from the ship's transducer. Immediately following the detection of this pulse, each bottom transponder generates a reply pulse at a specific frequency (11.5, 12.5 and 13.5 kHz). These reply pulses are detected by the ship's transducer. Slant ranges between the ship and each transponder are calculated using the one-way travel time and the local sound velocity profile, as detailed in CPP81 and CP81. The ship's position relative to the transponder net is computed using an operator-selected pair of slant ranges.

The sonobuoy cycle also begins with a pulse transmission from the ship's transducer. The reply pulses from the bottom transponders are received at the drogue and transmitted (via radio) to the ship. The travel time from each transponder to the drogue is found by subtracting the ship to transponder travel time (determined by the most recent ship cycle) from the total (ship to transponder to drogue) travel time. These travel times are converted to slant ranges and used to calculate the drogue position with respect to the transponder net.

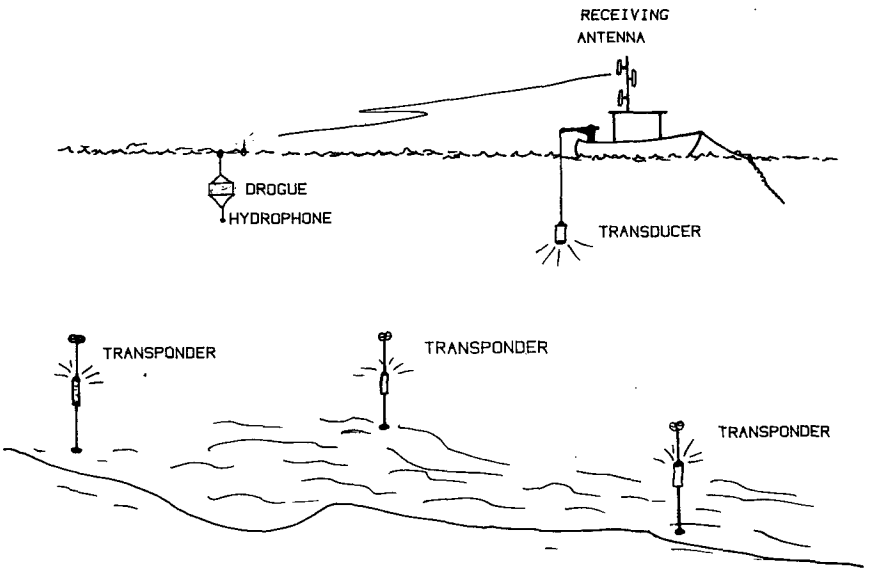

FIG. 5. Schematic sketch of the acoustic tracking system.

The baseline lengths between transponders and transponder depths are determined by a survey in which travel times are collected from a number of locations and analyzed using a least-squares technique. Geographic positioning of the transponder net is accomplished using the ship's navigation system (CP81).

The procedure of alternating between ship and sonobuoy cycles yields a drogue position one to two times a minute. The normal practice is to track each drogue for about 5 min at a time. The present system can concurrently track 16 drogues, each transmitting at a different frequency. The range of tracking varied from 4 to 8 km.

To our knowledge the acoustic navigation system has never been used in shallow, highly stratified water such as Lake Huron. Because of the acoustic ray bending in such an environment, first received pulses are often those of rays reflected from the bottom. The effects of ray bending on the accuracy and performance of the navigation system at Lake Huron has been examined in detail by Churchill (1981). It was found that ray bending had a minor contribution to velocity uncertainty (<2%), but a significant effect on tracking range.

b. Acoustic drogue design

The acoustic drogue assembly consists of a drogue of matted packing material, sonobuoy electronics enclosed within the drogue, an attached hydrophone and a float-antenna assembly.

A typical assembly of a drogue used during the low wave (0–0.6 m) conditions is shown in Fig. 6. The drogue is constructed of a wire mesh frame with a padding of 5 cm thick, densely entwined, synthetic horsehair fastened to the exterior. The float-antenna assembly consists of a support float for the drogue connected by 1.3 m of antenna wire (RG-174/U) to an antenna-bearing float. Both are 10 cm diameter × 15 cm long copper floats that drift with the top of the float approximately 7 cm above the water surface. The VHF electronics package has been modified to permit the use of a one-quarter wave antenna (0.16 cm diameter by 41 cm long). The electronics package consists of a modified Magnavox AN/SS041B so-

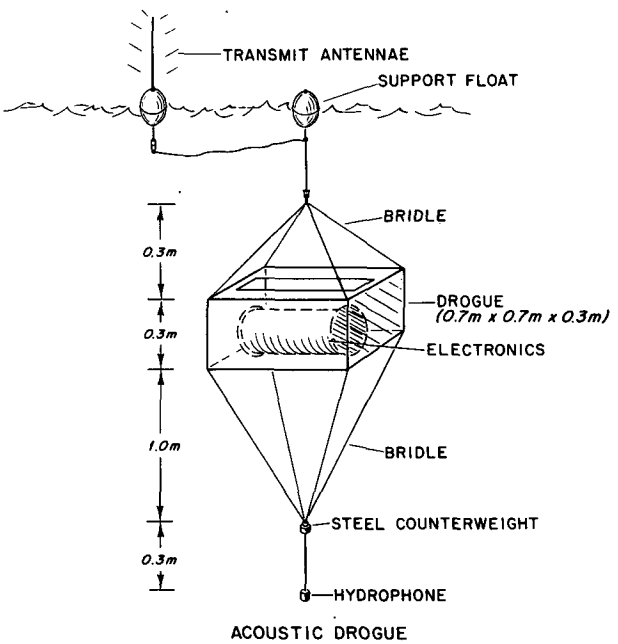

FIG. 6. A typical acoustic drogue assembly.

nobuoy radio in a 46 cm long by 13 cm diameter aluminum housing which is incorporated into the interior of the drogue.

Experiments during which dye was released from the center of a drogue drifting in a near-shore current showed no appreciable velocity between the drogue and the surrounding water.

c. Data analysis

Drogue and ship positions were calculated by a nonlinear regression technique which included all three slant ranges. Each position calculated by this method minimizes the quantity

$$SS = \sum_{i=1}^{3} (SL_i - sr_i)^2, \tag{4}$$

where SL_i is the slant range between transponder i and the drogue or ship hydrophone, as determined from the travel time. The computed slant range sr_i is given by

$$sr_i = [(Xsd - Xt_i)^2 + (Ysd - Yt_i)^2 + (Zsd - Zt_i)^2]^{1/2},$$

where Xsd and Ysd are the east and north position components of the ship or drogue; Zsd is the known depth of the hydrophone of the drogue or ship, and Xt_i, Yt_i, Zt_i are the coordinates of transponder i.

The square root of SS defines the slant range standard error for the particular fix. These values were used to identify and reject questionable fixes. The average value was ~40 m for drogue fixes and 10 m for ship fixes.

East and north drogue velocity components were taken as the slopes of regressions relating position component with time. For drogue tracks which were nearly straight, linear regressions were used. Velocity components of curved tracks have been computed from quadratic regressions. Standard errors of velocity about the regressions were calculated from the variance-covariance matrix [Draper and Smith (1966)] and ranged from 0.01 to 0.18 cm s^{-1}.

d. Results

At Lake Huron, drogues were released and tracked from Flag Station 8 of Fig. 3. Velocity profiles of a typical experiment are displayed in Fig. 7. All drogue velocities of Fig. 7 rotated at approximately half the inertial frequency of $2\pi/17$ h^{-1}; one should keep in mind, however, that drogues were tracked for less than 1/4 of an inertial period. At all times there was a well-defined relative velocity nearly aligned with the wind and wave direction.

Similar to visually tracked drogue and drifter velocities, acoustic drogue velocities appeared to consist of two components: a surface-layer current which was nearly parallel with the wind and wave propagation direction, and a subcurrent which rotated clockwise

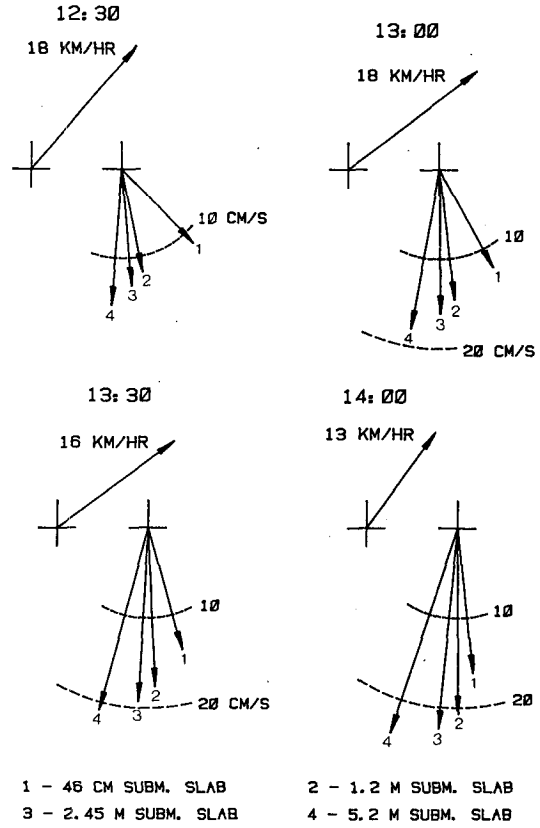

FIG. 7. Drogue and wind velocities of the 20 August 1980 experiment.

with time. The rotation of the subcurrent is typical of currents observed following a sudden change in wind stress and may be attributed to near-inertial oscillation or "Poincaré waves," (Mortimer, 1963), which have often been observed in this neighborhood (Murthy and Dunbar, 1981).

4. Discussion—The surface-layer current

a. Relation to wind speed and sea state

Several investigators have determined theoretically and experimentally in the laboratory and field the ratio of wind-induced surface velocity to the free-stream wind speed (or wind speed at some reference height, usually 10 m). Tsahalis (1979) has compiled a number of reported values which ranged from 0.026 to 0.045. In coastal waters the total surface velocity often contains a significant tidal or geostrophic component which is independent of the instantaneous wind. At such locations the wind-induced drift must be taken as the surface velocity relative to a depth which is just below the layer of direct wind influence.

Listed in Table 1 are velocities of the thinnest visually tracked drifter relative to the 1.8 m drogue. These are plotted against wind speed at 3 m in Fig. 8 (Lake Huron data only). Also plotted is a line which

TABLE 1. Velocities of shallowest and deepest visually tracked drifters, relative velocities (deepest to shallowest), and concurrent wind velocities.

From measurements in Cape Cod Bay

Drifter at 2.5 cm		Drogue at 1.8 m		Relative velocity (1.8 m to 2.5 cm)		Wind velocity	
Speed (cm s^{-1})	Direction (deg)	Speed (cm s^{-1})	Direction (deg)	Speed (cm s^{-1})	Direction (deg)	Speed (m s^{-1})	Direction* (deg)
36.1	285.	28.4	297.	9.8	252.	4.0	265.
36.0	293.	28.7	304.	9.6	258.	3.5	265.
27.6	281.	18.2	296.	11.0	255.	4.5	245.
22.9	277.	15.6	287.	8.0	257.	4.5	240.
18.3	246.	11.2	202.	13.0	284.	3.5	285.
19.2	251.	10.3	201.	14.9	283.	4.2	305.

From measurements in Lake Huron

Drifter at 1.2 cm		Drogue at 1.8 m		Relative velocity (1.8 m to 1.2 cm)		Wind velocity	
Speed (cm s^{-1})	Direction (deg)	Speed (cm s^{-1})	Direction (deg)	Speed (cm s^{-1})	Direction (deg)	Speed (m s^{-1})	Direction* (deg)
12.1	155.	5.3	213.	10.3	129.	6.3	159.
25.8	30.	18.0	27.	7.9	36.	5.6	25.
25.3	46.	17.7	59.	9.5	22.	5.6	31.
26.4	48.	17.7	70.	12.0	15.	6.7	44.
18.8	63.	13.2	71.	6.1	46.	<1.	46.
16.5	65.	11.4	71.	5.3	51.	<1.	46.
10.2	147.	2.7	206.	9.1	132.	4.7	144.
5.6	128.	4.3	251.	8.8	104.	3.3	136.
33.1	10.	24.9	14.	8.5	358.	7.2	4.
31.2	3.	26.8	13.	6.6	320.	6.9	354.
39.1	14.	32.3	16.	6.9	5.	8.1	4.
37.9	19.	31.7	25.	7.4	249.	6.9	4.
33.6	14.	28.7	29.	9.5	322.	7.7	354.
30.4	12.	20.7	12.	9.7	12.	3.3	54.
27.0	18.	18.7	14.	8.5	29.	4.7	20.
37.8	36.	29.8	41.	7.6	16.	5.0	11.
12.9	7.	8.3	32.	6.4	333.	2.8	324.
5.8	335.	3.6	189.	9.0	348.	4.6	334.

* Direction toward which the wind was blowing.

represents a ratio of relative velocity to wind speed equal to 0.03. Note that most relative velocities lie well below this line. Total wind-induced drift velocities are likely to be significantly larger than the relative velocities shown, however, because of the limited depth range of the sighted drogue observations. Fig. 7, for example, shows a shear velocity, which is parallel to the wind, extending to at least 5 m. Fig. 8 does not show any clear relation of relative velocity to wind speed, suggesting that factors other than just the wind speed influenced the relative velocities in the shallow (and fixed) depth range considered.

Another possible influence is the condition of the sea surface. During the tracking experiments only visual observations of waves were recorded. Unfortunately, these were not sufficiently detailed to infer significant wave heights. They have, however, been sorted into six "roughness" categories ranging from very calm to very rough, according to estimated dominant wave height and steepness. Relative velocities of Fig. 8 are graphed against sea state estimate in Fig. 9. There is an apparent increase of relative velocity with estimated sea state, although one should not place too much reliance on such a highly subjective result.

On first consideration it is puzzling that the relationship of relative velocity to subjectively judged sea state is so different from its relationship to wind speed. Due to the limited fetch at the experimental site, one would expect wind speed and perceived sea state to be directly related and thus have a similar relationship to the relative velocity. This was not the case, however, because waves were steep, even under low wind speeds, when the wind and mean current in the surface mixed layer were in opposite directions. This was often observed shortly after a reversal in the mean wind direction.

Although, as previously stated, the apparent in-

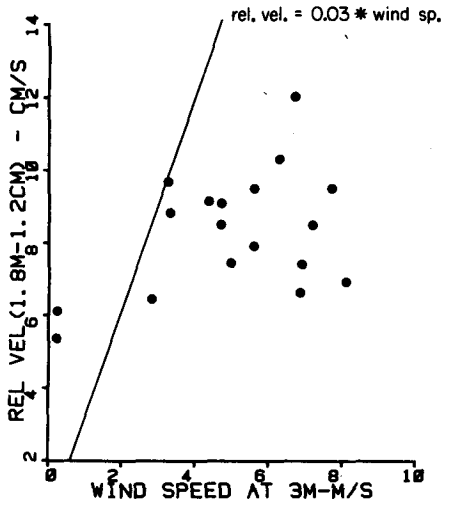

FIG. 8. Relative velocity magnitude of 1.2 cm drifter with respect to 1.8 m drogue against wind speed at 3 m.

crease of relative velocity with estimated sea state is highly subjective and thus subject to doubt, it is nonetheless of interest to consider possible reasons for the apparent relation. Two possibilities are:

1) In turbulent shear flow the relative velocity is proportional to friction velocity $u_* = (\tau_0/\rho_w)^{1/2}$, where τ_0 is the surface wind stress and ρ_w the water density. Observed "choppiness" may be a clearer indicator of wind stress than wind speed within the limited range of wind speeds in question.

2) Relative velocities may have been, at least on a number of occasions, primarily a manifestation of Stokes drift in nonlocally generated waves rather than of turbulent shear flow.

b. *Similarity to logarithmic-layer flow over a rough wall*

It has repeatedly been suggested (Shemdin, 1972; Wu, 1975; Jones and Kenney, 1977; Csanady, 1979) that shear flow near the air/water interface is analogous to turbulent flow over a rough surface. For such flow it is often assumed that there is a region adjacent to the surface where the stress can be considered constant. This region may possibly consist of two sublayers which are characterized by the velocity gradient. Laboratory studies of Wu (1975) have indicated that immediately below the free surface there is a very thin layer in which the velocity gradient is constant. In this layer the velocity gradient may be related to stress by

$$\frac{\partial u}{\partial z} = \frac{u_*^2}{\nu_e}, \tag{5}$$

where ν_e is an effective viscosity. Slightly below the free surface it has been shown that the velocity varies logarithmically with depth and is usually written in Nikuradse's (1933) form:

$$\frac{u_{R,0}}{u_*} = \frac{1}{k}\ln\left(\frac{z}{r}\right) + 8.5, \tag{6}$$

where $u_{R,0}$ is the velocity relative to the surface, k Kármán's constant, taken as 0.4, z the distance from the surface, and r the Prandtl–Schlichting equivalent sand grain roughness.

A typical profile of velocity relative to 1.2 cm ($u_{R,\,1.2\,\mathrm{cm}}$) versus logarithm of depth is shown in Fig. 10. For all sighted drogue profiles, there was a definite linear relation between $u_{R,\,1.2\,\mathrm{cm}}$ and ln(z) in the upper

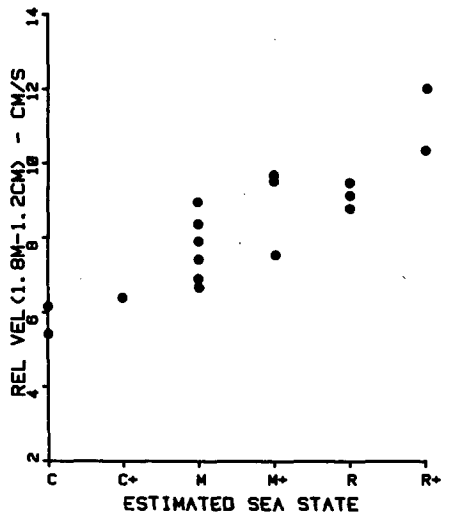

FIG. 9. Relative velocity magnitude of 1.2 cm drifter with respect to 1.8 m drogue against estimated sea state: calm (C); moderate (M); rough (R).

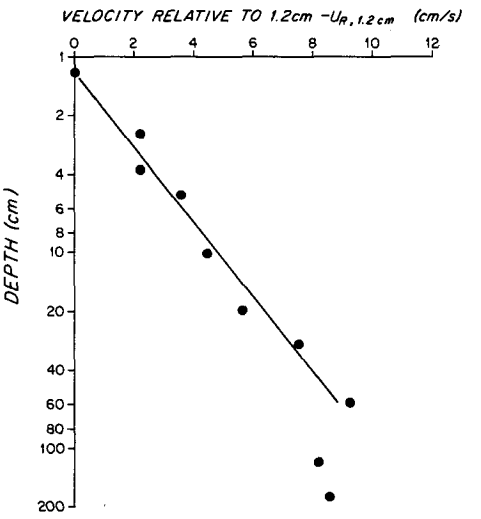

FIG. 10. Typical profile from sighted drifter and drogue data of velocity relative to 1.2 cm against depth (logarithmic scale). The line is from least-squares linear regression in the upper 60 cm.

60 cm ($R^2 > 0.93$ and generally $R^2 > 0.97$). Further below, velocities at 1.2 and 1.8 m differed from the least-squares linear relation by more than 1 cm s^{-1} in 70% of the observations.

Values of u_*, calculated from the least-squares fit of $u_{R,\,1.2\,\mathrm{cm}}$ versus ln(z) in the upper 60 cm, are listed in Table 2 and graphed against wind speed in Fig. 11. As with the relative velocity magnitudes, there is no clear dependence of u_* on wind speed. However, from the graph a mean ratio of $u_*/WS_{3\,\mathrm{m}} \simeq 1.33 \times 10^{-3}$ can be deduced, where $WS_{3\,\mathrm{m}}$ is the wind speed at 3 m. From this ratio a drag coefficient can be estimated by noting that

$$\tau_0 = \rho_a C_{3\,\mathrm{m}} WS_{3\,\mathrm{m}}{}^2 = u_*^2 \rho_w, \qquad (7)$$

where ρ_a is the air density, and $C_{3\,\mathrm{m}}$ the wind drag coefficient referred to the wind at 3 m. This drag coefficient is supposed to parameterize the wind stress transmitted by viscosity and small-scale fluctuating motion, excluding any horizontal force exerted by the airflow on longer wave components. The resulting estimate is $C_{3\,\mathrm{m}} = 1.5 \times 10^{-3}$, which is within the range of commonly quoted values, and demonstrates that realistic values of stress can be calculated from profiles below the water surface using (6) and a Kármán's constant of 0.4.

TABLE 2. Values of friction velocity, roughness length, effective viscosity and eddy Reynolds number calculated from visually tracked drogue and drifter profiles.

u_* (cm s^{-1})	r (cm)	ν_e (cm^2 s^{-1})	Re	Wind speed at 3 m (m s^{-1})
From measurements in Cape Cod Bay				
1.04	37.	1.6	25.	4.0
0.93	50.	2.0	23.	3.5
1.12	33.	1.5	24.	4.5
0.92	57.	1.7	31.	3.5
1.28	48.	2.7	23.	4.5
From measurements in Lake Huron				
0.90	21.	1.1	17.	6.3
0.64	33.	1.0	21.	5.6
0.88	30.	1.3	20.	5.6
1.21	22.	1.4	20.	6.7
0.50	22.	0.6	22.	<1.
0.31	24.	0.3	23.	<1.
0.94	46.	2.4	18.	4.7
0.87	45.	1.8	22.	3.3
0.90	23.	1.0	21.	7.2
0.83	26.	1.0	21.	6.9
1.03	22.	1.2	20.	8.1
0.60	12.	0.5	15.	6.9
1.04	25.	1.0	25.	7.7
1.03	17.	1.0	18.	3.3
0.63	23.	0.6	26.	4.7
0.64	24.	0.8	20.	5.0
0.55	32.	0.8	23.	6.4
0.51	41.	1.0	21.	2.8
0.48	25.	0.5	24.	4.4

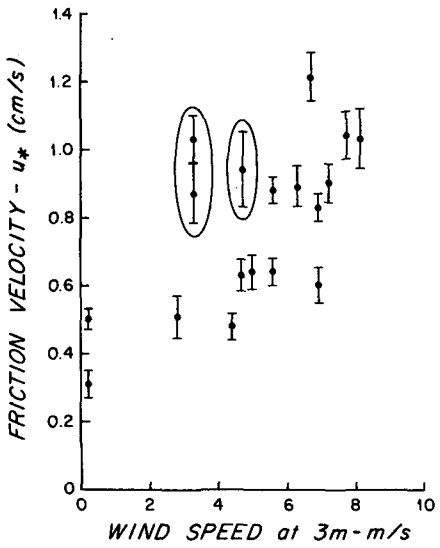

FIG. 11. Friction velocity, calculated from least-squares fit of $u_{R,\,1.2\,\mathrm{cm}}$ with ln(z), against wind speed at 3 m. Error bars are computed from standard errors of the least-squares fit; 95% confidence intervals are approximately 2.3 times larger. Enclosed values have been calculated from profiles measured during light winds and high swell.

The calculation of r requires relating the velocity profile to the surface velocity. There was no systematic curvature in observed relative velocity with depth in the uppermost 5.1 cm in Lake Huron (four observed levels: 1.2, 2.5, 3.8 and 5.1 cm). A near-surface velocity gradient was determined from these four velocities using the least-squares method. There were only two reliable velocities measured in the uppermost 5.1 cm in Cape Cod Bay. The Cape Cod Bay velocity profiles were referred to a surface velocity determined by quadratic extrapolation of the three velocities in the upper 10.2 cm (at 2.5, 5.1 and 10.2 cm).

From the estimated surface velocity gradient the near-surface effective viscosity can be calculated from (5). From u_*, r and ν_e an eddy Reynolds number may be formed:

$$\mathrm{Re} = \frac{u_* r}{\nu_e}. \qquad (8)$$

Computed values of r, ν_e and Re are listed in Table 2. The uncertainties of these quantities are large due to the relatively large standard errors of the surface velocity gradient. The order of magnitude should, however, be correct. The roughness length is of order 30 cm which is more than two order of magnitude greater than typical roughness lengths inferred from profiles on the air side of the air/sea interface as reported by Roll (1965). The large magnitude of these roughness lengths could be partially due to an underestimation of $u_{R,0} - u_{R,\,1.2\,\mathrm{cm}}$. A 4.5 cm s^{-1} underestimation would cause the calculated value of r

to be high by a factor of 10. As previously noted, confetti sightings were sparse and relatively unreliable (as indicated by high *ERR*2 values). The most trustworthy confetti velocities indicate that the least-squares estimates of $u_{R,0} - u_{R,\,1.2\,\mathrm{cm}}$ were in error by not more than 2 cm s^{-1}, which would, at most, result in a factor of 3 error in r.

c. *The importance of wave drift*

Investigators have differed as to the importance of wave-induced nearsurface drift. Bye (1967), Kenyon (1970) and Kirwan *et al.* (1979) proposed that the observed near-surface velocity gradient is primarily a manifestation of Stokes drift. From field and/or laboratory data, Keulegan (1951), Van Dorn (1953) and Shemdin (1972) concluded, on the other hand, that waves had little effect on near-surface drift.

In the absence of wind, the wave-induced drift magnitude in free sinusoidal gravity waves (Stokes drift) can be reliably calculated from the wave amplitude and frequency, as demonstrated by Alofs and Reisbig (1972) and Lange and Huhnerfuss (1978). Stokes drift of a random wave field is often estimated by summing the contribution of each Fourier component. Given a continuous frequency spectrum the estimate is

$$u_S = \frac{2}{g}\int_0^{F_u/2\pi} \sigma^3 W(\sigma)\exp(-2\sigma^2 z/g)d\sigma, \qquad (9)$$

where σ is the frequency (rad s^{-1}), W the wave energy per unit of frequency, g the gravitational acceleration, and F_u the upper frequency of integration (Hz).

Eq. (9) is derived on the assumptions that 1) the fluid is inviscid, 2) each sinusoidal wave component contributes to Stokes drift as a monochromatic wave, and 3) that these contributions can be superimposed linearly. These assumptions are certainly overidealized, but the calculation of a Stokes drift profile according to (9) should nevertheless give an indication of what may be expected in the absence of significant vertical mixing. The weakest assumption is that very short waves contribute to the integral in (9). Hence a cutoff at a moderately high frequency might be realistic.

Wave energy spectra, each computed from a 20 min record of a waverider accelerometer buoy moored in 11.3 m of water off Port Elgin, Ontario (approximately 20 km from the Lake Huron project site), have been provided to us by the Marine Environmental Data Service of the Canadian government. Fig. 12 shows estimates of Stokes drift calculated from two such spectra, together with an estimate calculated from a spectrum of a capacitance wave staff (Simpson, 1969). Also shown is the significant wave height of each spectrum which is approximately equal to the mean of the highest one-third number of waves (Longuet-Higgins, 1952), and roughly corresponds to the visual estimate of sea state. The profiles show an increase in inviscid wave drift with significant wave height. They also show that the Stokes drift estimate varies nearly logarithmically with depth to order 1 m depth, in agreement with the results of Bye (1967). Values of u_* computed by applying (6) to the logarithmic portions of these profiles are within a factor of 2 of values calculated from observed profiles with corresponding significant wave height.

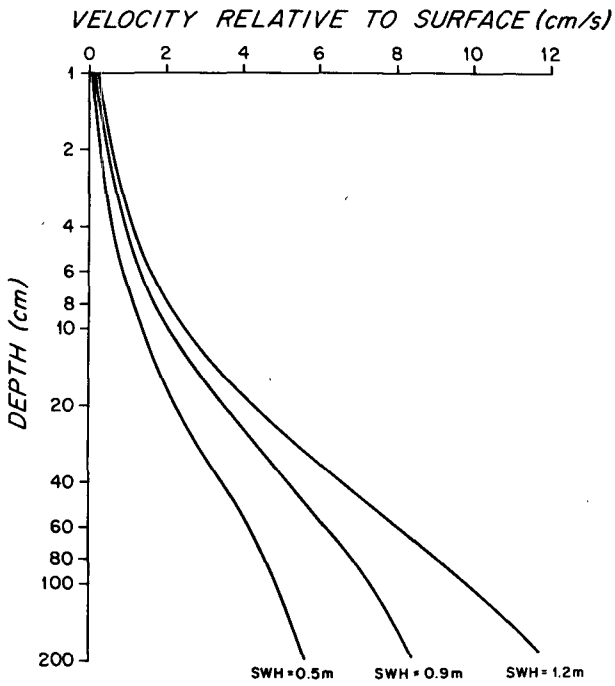

FIG. 12. Stokes drift estimates relative to the surface velocity against depth. Profiles with corresponding significant wave height (SWH) of 0.5 and 0.9 m were calculated from waverider spectra extrapolated to 1 Hz. The profile with SWH = 1.2 m was calculated using a spectrum from Simpson (1969).

Eq. (9) may be reasonably accurate under conditions of long, steady swell and light wind (little turbulence). Applying (6) to velocity profiles measured during such conditions may thus result in u_* values which are not representative of stress. u_* values computed from profiles taken during light wind and high swell are noted in Fig. 11 and do appear to be anomalously high.

Fig. 13 compares relative velocity profiles calculated from a spectrum with 0.9 m significant wave height with profiles measured during seas of about 0.9 m. The solid line profile was calculated with F_u equal to the waverider cutoff frequency of 0.5 Hz. The dashed line was calculated from the spectrum extrapolated to 1 Hz using the Phillips (1958) form of the equilibrium spectrum: $W(\sigma) = \beta\, g^2\, \sigma^{-5}$, with β calculated from spectral values near 0.5 Hz. Similar profiles were obtained from calculations using the spectra of Simpson (1969) which included the fre-

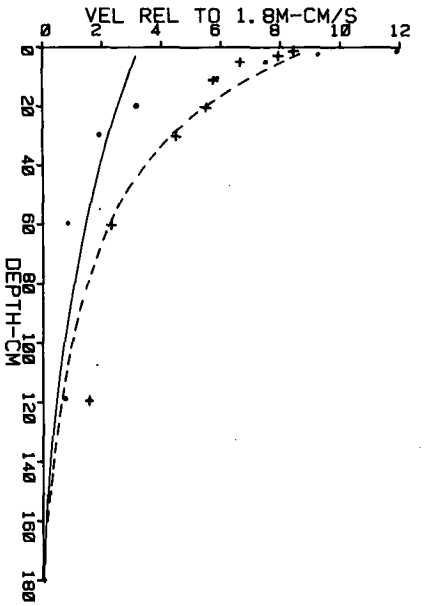

FIG. 13. Velocity profile relative to 1.8 m calculated with F_u in Eq. (9) equal to 0.5 Hz (solid line) and to 1 Hz (dashed line). Dots and crosses are profiles of two-sighted drogue/drifter experiments.

quency range 0.1 to 1 Hz (Fig. 12). This figure is not intended to be a comparison of observation to theory. It does indicate that the estimate of inviscid wave drift can be comparable to observed relative velocities if integration is carried out to a high frequency. From similar calculations Bye (1967) and Kenyon (1969) concluded that Stokes drift may, to a large extent, be responsible for near-surface drift. However, inclusion of frequencies much higher than the spectral peak is probably not justified.

In the presence of moderate to high winds, the Stokes drift profile is likely to be modified by turbulent mixing. Laboratory studies by Lange and Huhnerfuss (1978) have shown that velocity profiles produced by wind alone or wave action alone do not add linearly when both wind and waves are present. Nevertheless, it is important to note that the inviscid estimate of wave drift appears similar to turbulent shear flow with regard to dependence on sea state, logarithmic dependence with depth, and absolute magnitude. Stokes drift must therefore be considered when interpreting Lagrangian velocity profiles, especially those measured during conditions of light wind and high swell.

5. Conclusion

These experiments have demonstrated that near-surface mean Lagrangian velocities are nearly logarithmic with depth to order 1 m depth and that wind stress may be determined by the profile method using a Kàrmàn's constant of 0.4. The inferred roughness lengths are approximately two orders of magnitude greater than typical values on the air side of the air/sea interface. At low wind speeds, in the presence of swell, spuriously high surface stress may be inferred on account of the similarity of the Stokes drift profile to the velocity distribution in a turbulent wall layer.

Acknowledgments. Mr. Bert Pade was responsible for the development of the acoustic and sighted drogues and supervised much of the field work. Messrs. Ken Peal, John Loud and Stan Rosenblad modified the acoustic navigation system for drogue tracking. Paul-Andre Bolduc of the Canadian Marine Environmental Data Service generously supplied us with wave data.

This work was supported by the Department of Energy under Contract DE-AC02-79EV10005 and National Oceanic and Atmospheric Administration under Contract 03-50-022-26 and Grant 04-8-M01-62.

REFERENCES

Alofs, D. J., and R. L. Reisbig, 1972: An experimental evaluation of oil slick movement caused by waves. *J. Phys. Oceanogr.*, **2**, 439–443.

Bye, J. A. T., 1967: The wave-drift current. *J. Mar. Res.*, **25**, 95–102.

Churchill, J. H., 1981: Tracking nearsurface drogues using an acoustic travel time technique in shallow, highly stratified water: problems and observations. WHOI Tech. Rep. WHOI-81-37, 49 pp.

——, and B. H. Pade, 1980: Measurement of nearsurface current in Cape Cod Bay using sighted drogues. WHOI Tech. Rep. WHOI-80-8, 45 pp.

——, and ——, 1981: Acoustically and visually tracked drogue measurements of nearsurface water velocities in Lake Huron, plus observations of a coastal upwelling. WHOI Tech. Rep. WHOI-81-91, 122 pp.

——, —— and K. R. Peal, 1981: Water velocity measurement from nearsurface to 110 m depth at deep water dumpsite 106 using acoustically tracked drogues and conventional current meters. WHOI Tech. Rep. WHOI-81-11, 29 pp.

Csanady, G. T., 1979: A developing turbulent surface shear layer model. *J. Geophys. Res.*, **84**, 4944–4948.

——, 1981: Circulation in the coastal ocean. *Advances in Geophysics*, Vol. 23, Academic Press, 101–183.

Draper, N. R., and H. Smith, 1966: *Applied Regression Analysis.* Wiley, 407 pp.

Hunt, M. M., W. M. Marquet, D. A. Moller, K. R. Peal, W. K. Smith and R. C. Spindel, 1974: An acoustic navigation system. WHOI Tech. Rep. WHOI-74-6, 67 pp.

Jones, I. S. F., and B. C. Kenney, 1977: The scaling of velocity fluctuations in the surface mixed layer. *J. Geophys. Res.*, **82**, 1392–1396.

Kenney, B. C., 1977: An experimental investigation of the fluctuating currents responsible for the generation of windrows. Ph.D. dissertation, University of Waterloo, Waterloo, Ontario, 162 pp.

Kenyon, K. E., 1970: Stokes transport. *J. Geophys. Res.*, **75**, 1133–1135.

——, 1969: Stokes drift for random gravity waves. *J. Geophys. Res.*, **74**, 6991–6994.

Keulegan, G. H., 1951: Wind tides in small closed channels. *J. Res. Nat. Bur. Stand.*, **46**, 358–381.

Kirwan, A. D., G. McNally, S. Pazan and R. Wert, 1979: Analysis of surface current response to wind. *J. Phys. Oceanogr.*, **9**, 401–412.

Lange, P., and H. Huhnerfuss, 1978: Drift response of monomolecular slicks to wave and wind action. *J. Phys. Oceanogr.*, **8**, 142–150.

Longuet-Higgins, M. S., 1952: On the statistical distribution of the heights of sea waves. *J. Mar. Res.*, **11**, 245–265.

Mortimer, C. H., 1963: Frontiers in physical limnology with particular reference to long waves in rotating basins. Publ. No. 10, Great Lakes Res. Div., University of Michigan, 9–42.

Murthy, C. R., and D. S. Dunbar, 1981: Structure of the flow within the coastal boundary layer of the Great Lakes. *J. Phys. Oceanogr.*, **11**, 1567–1577.

Nikuradse, J., 1933: Stronungsgasetze in rauhen Rohren. *VDI Forschungsheft*, No. 361.

Phillips, O. M., 1958: The equilibrium range in the spectrum of wind-generated waves. *J. Fluid Mech.*, **4**, 426–434.

Roll, H. U., 1965: *Physics of the Marine Atmosphere.* Academic Press, 426 pp.

Shemdin, O. H., 1972: Wind-generated current and phase speed of wind waves. *J. Phys. Oceanogr.*, **2**, 411–419.

Simpson, J. H., 1969: Observations of the directional characteristics of sea waves. *Geophys. J. Roy. Astron. Soc.*, **17**, 93–120.

Spindel, R. C., and R. P. Porter, 1974: Precision tracking system for sonobuoys. *IEEE Ocean 74 Symposium*, Halifax, Nova Scotia, Vol. 2, 162–165.

Tsahalis, D. T., 1979: Theoretical and experimental study of wind- and wave-induced drift. *J. Phys. Oceanogr.*, **9**, 1243–1257.

Van Dorn, W. G., 1953: Wind stress on an artificial pond. *J. Mar. Res.*, **12**, 249–276.

Wu, Jin, 1975: Wind-induced drift currents. *J. Fluid Mech.*, **68**, 49–70.